2013

Raman Micro Spectroscopy Study of the Interaction of Vincristine with A549 Cells Supported by Expression Analysis of bcl-2 Protein

Haq Nawaz
Technological University Dublin

Amaya Garcia
Technological University Dublin

Aidan Meade
Technological University Dublin, aidan.meade@tudublin.ie

See next page for additional authors

Recommended Citation

Byrne, H. J. (2013) Raman micro spectroscopy study of the interaction of vincristine with A549 cells supported by expression analysis of bcl-2 protein", *Analyst,* 138, pp.6177-6184. doi: 10.1039/c3an00975k

Funder: HEA

ARTICLE TYPE www.rsc.org/xxxxxx | XXXXXXXX

Raman micro spectroscopy study of the interaction of vincristine with A549 cells supported by expression analysis of bcl-2 protein

Haq Nawaz[a,c]*, Amaya Garcia [a], Aidan D. Meade[a,b], Fiona M. Lyng[a] , Hugh J. Byrne[b]

[a]. DIT Centre for Radiation and Environmental Science (RESC), Focas Research Institute, Dublin Institute of Technology, Kevin Street, Dublin 8, Ireland
[b]. Focas Research Institute, Dublin Institute of Technology, Kevin Street, Dublin 8, Ireland.
[c] National Institute for Biotechnology and Genetic Engineering (NIBGE), P.O.Box 577, Jhang Road Faisalabad, Pakistan.
*Corresponding Author (a, c):
Haq Nawaz,
DIT Centre for Radiation and Environmental Science (RESC), Focas Research Institute, Dublin Institute of Technology, Kevin Street, Dublin 8, Ireland.
&
National Institute for Biotechnology and Genetic Engineering (NIBGE), P.O.Box 577, Jhang road Faisalabad, Pakistan.

haq.nawaz@dit.ie

Received (in XXX, XXX) Xth XXXXXXXXX 200X, Accepted Xth XXXXXXXXX 200X
First published on the web Xth XXXXXXXXX 200X
DOI: 10.1039/b000000x

Abstract

Understanding the interaction of anticancer drugs with model cell lines is important to elucidate the mode of action of these drugs as well as to develop cost effective and rapid screening methods. Raman spectroscopy has been demonstrated to be a valuable technique for high throughput, noninvasive analysis. The interaction of vincristine with a human lung adenocarcinoma cell line (A549) was investigated using Raman micro spectroscopy. The results were correlated with parallel measurements from the MTT cytotoxicity assay, which yielded an IC_{50} value of 0.10 ± 0.03 μM. The Raman spectral data acquired from vincristine treated A549 cells was analysed to understand its interaction with the nucleus in the cell and elucidate DNA intercalation. The dose dependent spectral changes in the nucleus are analysed by PLS-Jack knifing for the identification of the more significant changes associated with the mode of action of the drug. Results are correlated with a similar dose dependent expression analysis of the bcl-2 protein, an anti-apoptotic protein associated with DNA damage, in the vincristine treated A549 cells using flow cytometry. The results indicate the co-existence of two modes of action, microtubule binding at low doses and DNA intercalation at high doses.

Introduction

The *in vitro* study of the interaction of anticancer drugs with mammalian cells is important to elucidate the mechanisms of action of the drug on its biological targets and thereby maximise efficacy. Cancer cell lines can be a good model to study the effects of these anticancer agents and such *in vitro* studies are in accordance with the EU policy of Reduction, Replacement and Refinement (RRR) of the protection of animals used for experimental and scientific purposes (Directive 2010/63/EU). Another concern is the requirement of a non-invasive, cost effective, rapid screening technique which can analyse the samples, ideally without any labelling. Raman micro spectroscopy potentially provides these benefits [1]. In addition, Raman spectroscopy can provide high content information, as it can examine spectral changes in the cell membrane, cytoplasm and nucleus of the target cells simultaneously and can differentiate the biochemical interaction of external agents with the cell from its physiological response [2, 3].

The potential of confocal Raman micro spectroscopy (CRM) for the analysis of biological tissue [4] and the effect of external agents on the cell [5-9] has been demonstrated. Moreover, the technique, with its counterpart Fourier transform infrared (FTIR) micro spectroscopy, is being used to explore sub-cellular biochemical structure, as demonstrated by its use in studies investigating the action of various agents on biological macromolecules as well as their interaction with cancer cells [1-3, 10-17].

The use of CRM in studying the biochemical effects of established, commercially available anticancer drugs may be helpful therefore in order to validate its use for the evaluation of the novel anticancer agents. To this end, such an approach was demonstrated for the action of cis-platin with lung cells *in vitro* [2, 3]. The study utilized multivariate regression and feature selection techniques to correlate spectral changes with drug dose and cell viability, as measured using a standard cytotoxic assay.

A proposed primary mode of action of vincristine is through its binding to tubulin monomers in the cytoplasm, which leads to a change in the dynamics of the microtubule assembly and prevention of the formation of bi-polar spindles [18], necessary for the proper segregation of the duplicated chromosomes and ultimately cell division.

Additionally, however, vincristine has been reported to interact directly with DNA in acellular studies, as observed using techniques such as Atomic Force Microscopy [19], Fluorescence image microscopy [20] and FTIR spectroscopy [21], which indicate that it acts as an intercalator. The combined evidence raises the question as to whether vincristine causes cell death only by disturbing the dynamics of the microtubule assembly or whether the DNA damage caused by this anticancer agent also contributes to its efficacy.

The purpose of this study is to further elucidate the interaction of the drug on a cellular level, as well as the cellular response pathways, using CRM to characterise biochemical changes on the subcellular level. To support the spectroscopic investigation, the expression of bcl-2 protein as a result of vincristine treatment is explored using flow cytometry. Bcl-2 is an anti-apoptotic protein which is generated as a direct result of DNA damage, and is thus involved in the regulation of cell death and serves as an indicator of genotoxic stress to the cell [22, 23]. The comparison of the observations of changes to the Raman signatures of nucleus of the A549 cells as a result of vincristine exposure as compared to the unexposed control, as well as the changes in the expression profile of bcl-2, may lead to elucidation as to whether DNA damage contributes to the mode of action of this anticancer agent.

Experimental

MTT assay

Vincristine was purchased from Sigma Aldrich, Ireland, in the form of vincristine sulphate (V8388) and a stock solution was prepared in distilled water. Working solutions were prepared in the cell culture media.

MTT was obtained from Sigma Aldrich, Ireland. The MTT assay was performed in triplicate according to a method reported previously [24] with a slight modification. The exposure of A549 cells to vincristine was done for 96-hours, over a wide range of concentrations (0.01-10 μM) to establish the half maximal inhibitory concentration (IC_{50}) and the appropriate range over which to conduct the analysis.

The MTT measurement protocol was as follows. Cells were cultured in 96-well plates (Nunc, Denmark) at a density of 2×10^3 cells per well in Dulbecco's Modified Eagle Medium-F12 (DMEM) with all the supplements as listed above. After 24 hrs of initial cell attachment, the plates were washed with 100 μl/well phosphate buffered saline (PBS) and were treated with varying concentrations of vincristine in the range of 0.01 μM -10 μM (including a separate unexposed control sample). Following a 96-hour exposure period, the cells were rinsed with PBS and 100 μl of fresh medium (without supplements) were added to each well. A volume of 10 μl of MTT (5mg/ml) prepared in PBS was then added to each well and the plates were incubated for 3 hrs at 37 °C in a 5% CO_2 humidified incubator. After this incubation period, the medium was discarded, the cells were washed with 100 μl of PBS and 100 μl of Dimethyl Sulphoxide (DMSO) were added to each well to extract the dye. The plates were then shaken 240 times per minute for 10 min and the absorbance was measured at 570 nm using a micro plate reader (Tecan Genios, Grodig, Austria). Six replicate wells were used for each exposure.

Raman micro spectroscopy

In this work, CRM was conducted with a Horiba Jobin-Yvon, LabRam HR800 instrument using a 785 nm laser as source. Spectra were taken in the range from 600 cm^{-1} to 1800 cm^{-1} with a confocal hole diameter of 100μm. A x100 water immersion objective was used to focus the laser on the sample, immersed in 0.9% saline, yielding a spot size of ~1 μm.

For CRM, cell samples were cultured on quartz substrates according to a protocol outlined elsewhere [9]. Briefly, quartz coverslips were coated with a 2% w/v gelatin-water solution and maintained at 4 °C for 6 hrs to allow polymerization of the gelatin on the substrate. Subsequently, 2.5×10^3 A549 cells were attached to the substrates for a 48 hour period, and were exposed to vincristine concentrations in the range of 0.01 μM -10 μM for a 96-hour period (together with a non-exposed control sample). After the exposure period, the cells were fixed in 4% formalin for 10 minutes and were stored in 0.9 % physiological saline solution at 4 °C until the Raman analysis was performed [25]. All samples were prepared in triplicate.

For spectral acquisition, the laser power was approximately 70 mW at the sample. Spectra were taken in the range from 600 cm^{-1} to 1800 cm^{-1} with a confocal hole diameter of 100μm. A ×100 water immersion objective was used to focus the laser on the sample, immersed in 0.9% saline, yielding a spot size of ~1 μm. Multiple spectra were recorded from the nuclear portion, visually identified using the optical microscope of the instrument, of a total of 60 cells at each exposure level. The point spectra were recorded from the cell nuclei of the sixty different A549 cells for control as well as exposed samples.

Data analysis

All spectral analysis was performed in the Matlab 7.2 (The Mathworks Inc.) environment employing the PLS Toolbox 5.0.3 (Eigenvector Research, Wenatchee, WA) and algorithms developed in-house. Subsequently, the spectra were smoothed with a Savitsky-Golay filter (order 5, 13 point window), and the quartz signal background was subtracted using algorithms developed in-house. Prior to

analysis, the spectra were also vector normalized and a fifth order polynomial was fitted to the spectra to remove any residual spectral baseline. Outlying spectra were removed using Grubb's filtering [26].

PLS Jack-knifing was employed as a multivariate feature selection technique [27-29]. The PLS regression algorithm seeks to develop a model that relates the spectral data (*X-matrix*) to a series of targets (*Y-matrix*, e.g. concentration of reaction product or analyte) according to the equation $Y=XB+E$, where B is a matrix of regression coefficients and E is the regression residual. The Y-matrix here consisted of values of the concentration of vincristine to which the cells were exposed, or the measured level of cell viability from the MTT assay. The PLS *Jack-knifing* method developed by Westad and Martens was then used to determine the spectral features that were statistically significant at a particular level of confidence using t-testing of the regression coefficients, B [29]. The Raman band assignments used in interpretation of the spectral features were taken from the literature [9, 15, 30-32].

Flow cytometry

For the culture of A549 cells, the materials and protocols used were the same as those described above for Raman spectroscopy measurements. The bcl-2 antibody labelled by FITC with an IgG1 isotype control was purchased from BD biosciences (BD 556357). The cytoperm/ cytofix fixation/ permeabilization kit was purchased from BD biosciences (BD 554714).

The A549 cells were cultured in tissue culture flasks (Nunc, Denmark) at a density of 1×10^5 cells in DMEM-F12 medium with all the supplements as described earlier. After 24 hrs of initial cell attachment, the plates were washed with PBS and were treated with varying concentrations of vincristine in the range from 0.01 µM-10µM (including a separate unexposed control sample). Following a 96-hour exposure period, the cells were trypsinised and collected in an Eppendorf, $1x10^6$ cells per sample. The cells were washed twice with ice cold Dulbecco's Phosphate-Buffered Saline (DPBS) buffer (containing protein and NaN_3), gently resuspended and centrifuged (250-300 g). The fixation buffer (250µl) was added to each sample, and the process was followed by gentle pipetting and incubation for 30 minutes at 4 ˚C. The fixed cells were washed and suspended in the stain buffer. This was followed by the addition of 100 µl of the permeabilization buffer and incubation for 15 minutes at room temperature. The samples were then washed twice with 1ml of the *perm wash* buffer and centrifuged at 250-300 g for 5 minutes at 4 ˚C, and the cells were suspended in 50 µl of the *perm wash* buffer and the diluted antibody was added. This was followed by incubation of the samples for 60 minutes, on ice and in the dark. Then cells were washed twice with the *perm wash* solution to remove the unbound antibody. The tubes were inverted and blotted to remove the supernatant. The samples were resuspended in stain buffer and analyzed by flow cytometry.

The expression analysis of the bcl-2 protein in A549 cells due to the action of the vincristine was performed using a Partec Flow Cytometer (Partec UK Limited, U.K.) and the data analysis was performed using Summit software (Version 4.3, DAKO, Denmark).

Results

IC_{50} for vincristine

The MTT results for the cytotoxicity measurement of vincristine in A549 cells are presented in **Figure 1**. The level of viability in each sample was normalised to that of the control sample. The Inhibitory Concentration (IC_{50}) value was derived from the data by a fit of the Hill equation, f(x) = min + (max-min)/(1+(x/IC_{50})^n) and found to be 0.10±0.03 µM. The primary purpose of the MTT assay was to determine the exposure range over which the maximum variation occurs in the cellular response, and thus the optimum range to probe the associated changes to the spectral response.

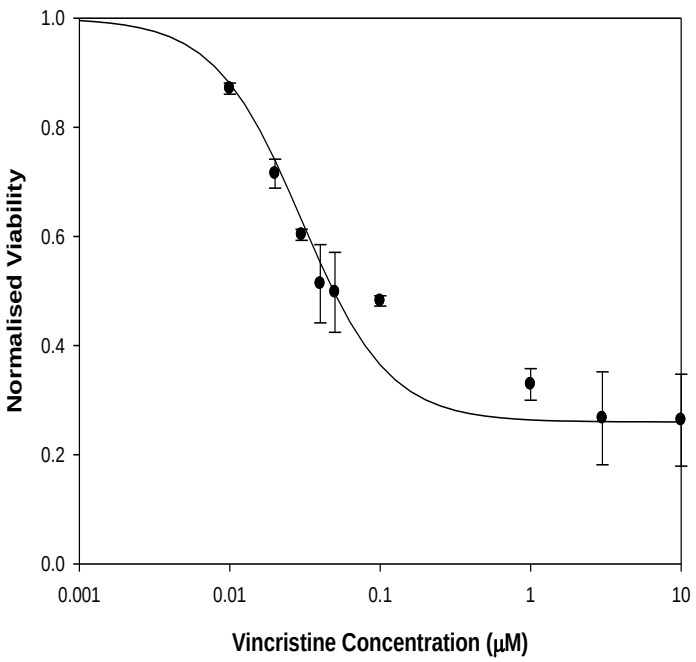

Figure 1 Viability of the A549 cells measured by MTT absorbance at 96 hours after exposure to vincristine. Error bars denote the standard error on the mean at each concentration.

Interaction of vincristine with the nucleus of A549 cells

To identify any biochemical changes caused by the direct action of vincristine on the nucleus, the Raman spectra of the nucleus of A549 cells exposed to the range of concentrations of vincristine were recorded. The nuclear

spectra of the mean control, and vincristine exposed samples are shown in **Figure 2**. The major changes observed in the spectra of the nucleus of A549 cells are in the Raman bands of the DNA bases, including thymine (669 $cm^{-1}$and 1253 cm^{-1}), adenine (728 cm^{-1}), guanine (1317 cm^{-1}) and cytosine (783 cm^{-1}). These changes can be attributed to the action of the vincristine within the nucleus of the A549 cells and specifically due to interaction with the DNA. As the concentration of the drug exposure increases, a decrease in the intensities of the bands associated with the DNA bases is observed. This is consistent with the results of the intercalation of the ethidium bromide, a well known DNA intercalator, into calf thymus DNA studied by Raman spectroscopy [33].

Conversely, [21] have reported an increase in the intensities of the bands due to DNA bases while investigating the effect of very high concentrations, ranging from 200-300 μM, of vincristine on calf thymus DNA, acellularly, with the help of FTIR spectroscopy. It should be noted, however, that these concentrations are significantly higher than the maximum of the range employed in this study (10 μM), and the clinically relevant IC_{50} (0.1 μM). The decrease in the intensities of the vibrational features ascribed to these DNA bases and most importantly the conformational changes of the B-form DNA into A-form, as indicated by the continuous decrease in the intensity of the Raman band at 827 cm^{-1} and concomitant increase in the intensity of the A-form DNA (811 cm^{-1}), due to the action of vincristine, provides evidence of intracellular intercalation of vincristine into the DNA. Moreover, in the control spectra of the nucleus of A549 cells, the CH_2 scissoring mode, observed as a sharp band at 1422 cm^{-1}, is considered as an important Raman marker of the B-form DNA and is found to be much more broader and lower in peak intensity in the A-form DNA [34]. This trend is clearly observable in the decreased contributions of this band in exposed samples in **Figure 2,** again indicating conformational changes in the B-form DNA in favour of the A-form.

Interestingly, in comparison to the effects on the nuclear Raman spectrum as a result of exposure to cisplatin, a known DNA groove binder, [2], the changes observed in the conformation of the B-form of DNA, the dominant form of cellular DNA, are more prominent. These changes, including decreases in the Raman intensities of the bands due to DNA bases and changes in the DNA conformation are the important Raman markers of DNA intercalation [33, 35-37]. Changes in the phosphodiester linkages, the O-P-O stretching vibrations of the DNA, are also observed at 1095 cm^{-1} along with a shift towards lower wavenumber at the higher concentrations including 3 and 10 μM. These changes indicate that vincristine also has the ability to bind to the DNA externally, in addition to its insertion into the DNA helix [21], as observed in the case of cisplatin studies [2]. Raman bands related to proteins are also observed, including those at 699 cm^{-1} and 718 cm^{-1}, 879 cm^{-1}, 1556 cm^{-1} (tryptophan ring breathing), 1265 cm^{-1} (amide-III, α-helix), 1302 cm^{-1} (CH_2 deformation), and 938 cm^{-1} (C-C stretching), 959 cm^{-1} (CH_3 deformation) and 1060 cm^{-1} (C-N stretching). The intensities of all these Raman bands increase as a result of an increase in the concentration of the exposures of the vincristine, particularly at the higher concentrations of this anticancer drug. This may be due to the fact that, after the conformational changes caused in the DNA by the anticancer drug binding, high mobility group proteins bind to the intercalation site and prevent repair by nuclease enzyme excision [38]. Furthermore, the proteins which are present in the nucleus, essentially required for the DNA strand packaging, may be more exposed due to the DNA strand opening which is caused by the intercalation of the vincristine.

It should be noted that the Raman spectral changes observed in **Figure 2** and discussed above can not unambiguously be attributed specifically to either the direct chemical binding of the vincristine to the DNA in the nucleus of the A549 cells or the subsequent physiological response of the cells to the drug. Therefore, PLS-Jack knifing was employed in an attempt to differentiate the chemical and the physiological effect of the drug by regressing the Raman spectral data from the nucleus of A549 cells against the exposure concentrations, compared to a similar regression against the cell viability end points [2].

PLS-Jack knifing analysis was carried out on the Raman spectral data from the nucleus of control and exposed A549 cells (over the full dose range) to further understand and confirm the mode of action of vincristine as an intercalative agent with DNA, and to identify the fingerprints of this interaction within the cellular spectra of exposed cells. The regression co-efficients were obtained by PLS-Jack knifing for separate regressions against vincristine concentrations and against the cell viability, as determined using the MTT assay. To reveal spectral changes that are most statistically significant with respect to regression against either endpoint, a t-test ($p<0.001$) was applied to the PLS-Jack knifing results, and the spectral features identified by this process are highlighted by vertical bands in **Figure 3**. The spectral bands identified and their assignments are tabulated in the Supplementary Information. The PLS regression of the nuclear data against vincristine concentrations identified a number of spectral features, labelled in **Figure 3 A,** related to the DNA bases, including guanine (1209-1211 cm^{-1}, 1289-1309 cm^{-1}, 1320-1322 cm^{-1}), thymine (673-678 cm^{-1}, 733-737 cm^{-1}, 1251-1257 cm^{-1}, 1378-1381 cm^{-1}) and cytosine (773-778 cm^{-1}, 1166-1173 cm^{-1}, 1298-1309 cm^{-1}). These features are identified only in the regression against the concentration of the vincristine. Moreover, changes associated with the phosphodiester linkage, O-P-O of the DNA, are also highlighted (1062-1065 cm^{-1} and 1075-1090 cm^{-1}), confirming the indications from **Figure 2** that vincristine, in addition to the intercalation mode of action, can also bind to the DNA externally.

The changes which are observed only in the regression of the nuclear data against cell viability, **Figure 3 (B)**, include C-C stretching of tyrosine residues (637-643 cm^{-1}), tryptophan ring breathing (696-700 cm^{-1}), amide-III (1250-1256 cm^{-1}), CH in plane bending of tyrosine (842, 844 cm^{-1}, 1176-1177 cm^{-1}) and CH deformation (1340-1343 cm^{-1}), which can be assigned to proteins. These features potentially originate from the high mobility group proteins which are activated to prevent further damage to the cell and to repair by nuclease enzyme excision [38].

Comparing the regression co-efficients obtained by PLS-regression analysis of the Raman spectral data against the

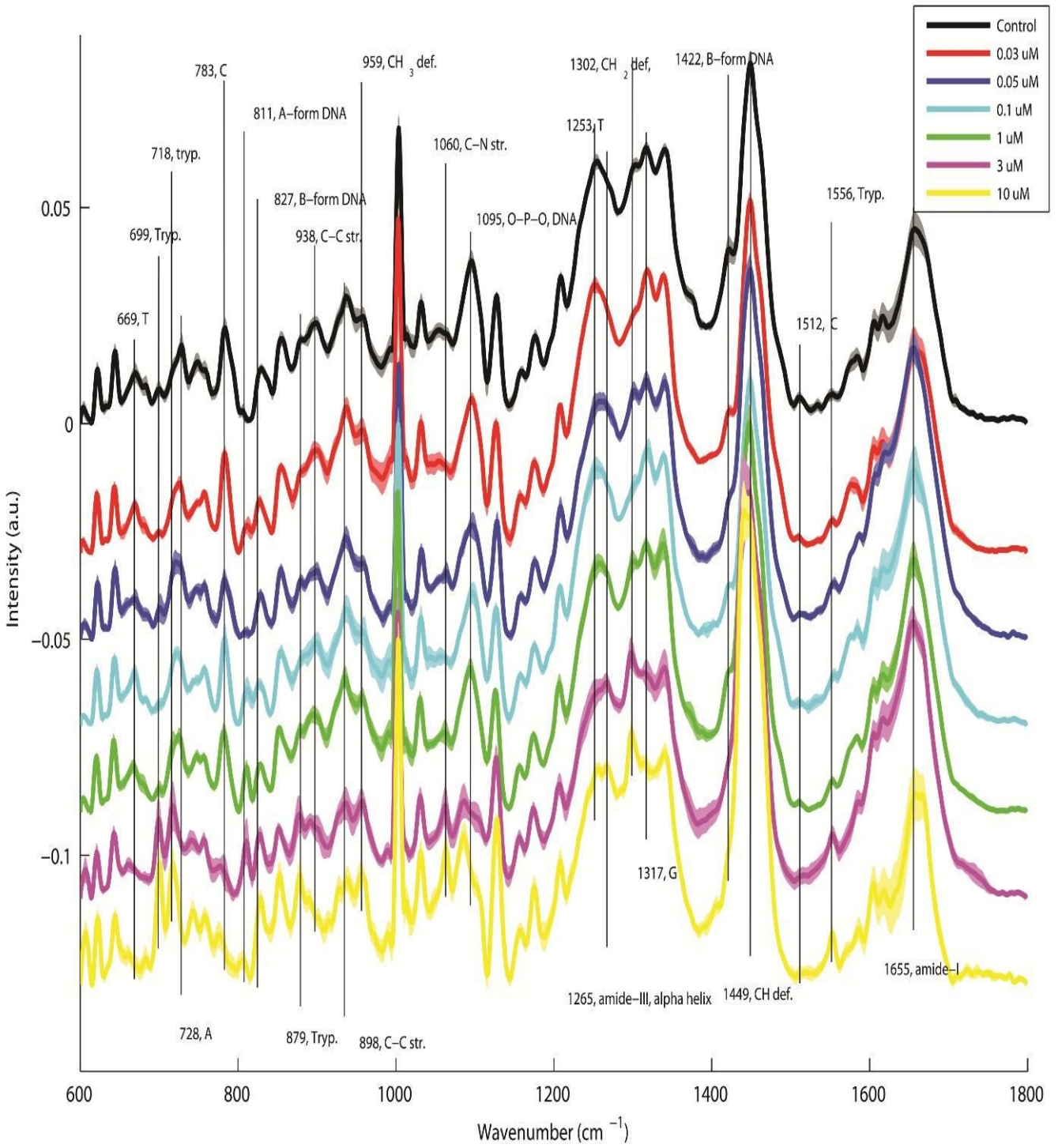

Figure 2: Mean spectrum of the nucleus of control and exposed A549 cells to 0.01-10 μM vincristine.

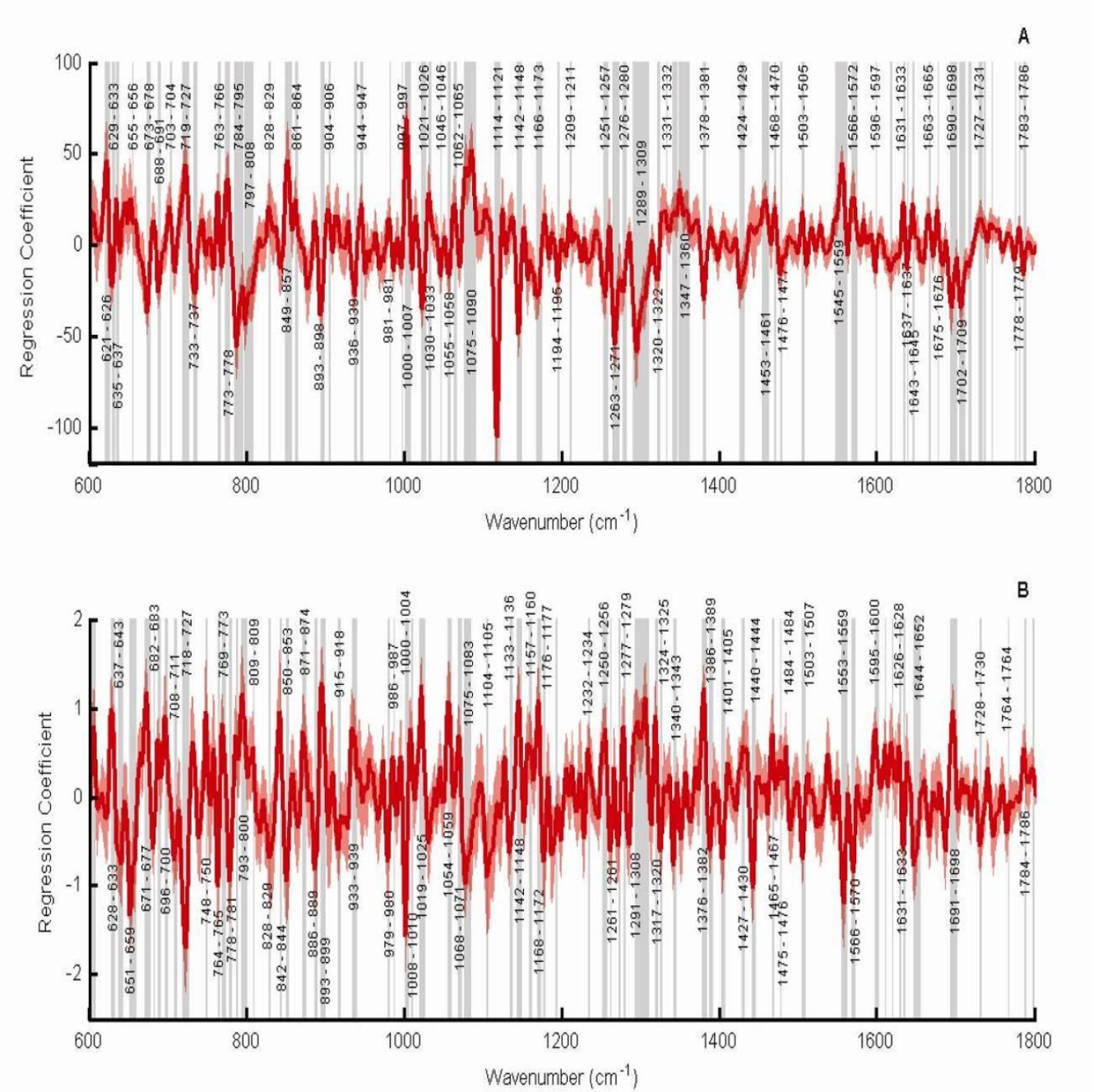

Figure 3 Feature selection in PLS-Jack knifing of Raman spectra of the A549 cell nucleus against (A) vincristine concentrations and (B) against cellular viability. The shaded areas in grey denote the statistically significant features selected using PLS Jack-knifing with a t-test ($p<0.001$) of regression coefficients (shown in red with associated standard error shaded about them). This demonstrates that the spectral data contains features associated with the biochemical effect of vincristine on the nucleus (A) and the associated effect on cellular viability (B).

concentrations of the exposures of the vincristine (which highlight the primary biochemical effect of the action of the agent) with those obtained via regression against cell viability (which highlight biochemical markers of the change in the viability of the cell), very different spectral features are selected as being statistically significant. This allows the differentiation of the biochemical changes caused in the A549 cells due to the DNA binding of the vincristine from the physiological response of the cells. It is noted that the PLS-Jack-knifing identifies a range of spectral features of relevance in the regression against each set of targets, the relevance of which appears statistically justified by the application of the t-test of the regression coefficients. Karaman et al. have however demonstrated that, in comparison to Sparse PLSR, the PLS- Jack knifing method was prone to selecting uninformative variables [39]. Ultimately the accuracy, sensitivity and specificity of the method should be validated using simulated datasets [12].

It is also noted that as a function of concentration, the cells which remain alive and are therefore probed by CRM potentially include those which have not yet been exposed, or have not yet responded to the drug, at low concentrations and potentially cells which are immune at higher concentrations. Nevertheless, the MTT assay is a measure of mitochondrial activity of the cell population, and the spectral markers identified by regression of the CRM data against the MTT target should provide a similar measure of this as an indication of viability for in vitro screening, in a label free manner. Ideally, to examine the true cellular response, CRM should be performed on live cells with subcellular resolution in a time resolved fashion.

Expression of bcl-2 protein in A549 cells treated with vincristine analysed by Flow cytometry

Raman spectroscopic analysis of the nucleus of exposed cells clearly indicates the interaction of vincristine with nuclear DNA. The bcl-2 protein is an anti-apoptotic protein [40, 41], and is involved in blocking DNA damage induced apoptosis [42, 43]. Changes in the expression of bcl-2 after exposure of the A549 cells to vincristine would indicate the involvement of the DNA damage pathway in the mode of action of the drug. Enhanced expression would point towards the development of resistance towards DNA damage induced cell death and decreased expression vice versa. Therefore, simultaneous observation of bcl-2 as a result of DNA damage and reduced cellular viability would point towards alternative mechanisms of cell death.

The results of flow cytometry for the expression of bcl-2 protein in A549 cells as a result of the treatment with various concentrations of vincristine ranging from 0.01 µM-10 µM, are shown in **Figure 4**. The results show that, due to the exposure of different concentrations of vincristine to A549 cells, the level of bcl-2 protein compared to control increases steadily up to a concentration of 5 µM, whereupon it decreases. These results indicate the involvement of the bcl-2 protein and therefore DNA damage in the mode of action of vincristine. A549 cells do not intrinsically express marked levels of bcl-2 protein as shown by [23, 44]. The up-regulation of the bcl-2 protein is therefore a response of the cell to the external agent which causes damage to the nuclear DNA. A similar expression profile, up regulation followed by down regulation of the bcl-2 protein, was observed while studying the effect of the anaesthetic halothane, considered as a DNA damaging agent, on A549 cells and this expression profile has been reported to be responsible for the resistance to apoptosis at low doses, whereas induced apoptosis due to DNA damage becomes prominent upon down regulation of bcl-2 at high doses [23]. In the current study, the Raman spectral data also indicates that vincristine binds to the cellular DNA by intercalation, so here bcl-2 up regulation may be in response to the DNA damage caused by the drug [45]. This may lead to the conclusion that vincristine also binds to DNA by intercalation, causes up regulation of bcl-2, whose anti-apoptotic function helps to delay the response of the cells at low doses (development of resistance). The bcl-2 expression is observed to decrease at doses > 5 µM, however, indicating that above these doses the cells are susceptible to apoptosis induced by DNA damage.

The Raman results give a clear indication that the documented acellular interactions of vincristine with DNA also occur intracellularly. However, the bcl-2 results indicate a resistance to apoptosis induced by DNA damage at vincristine doses <5 µM. Critically however, this dose is significantly higher than the IC_{50} value of 0.10 ± 0.03 µM, measured by the MTT assay. Therefore, the dominant mechanism of cell death at lower doses cannot be ascribed to DNA damage, but rather to the mechanism of tubulin binding leading to a change in the dynamics of the microtubule assembly and prevention of the formation of bi-polar spindles [18].

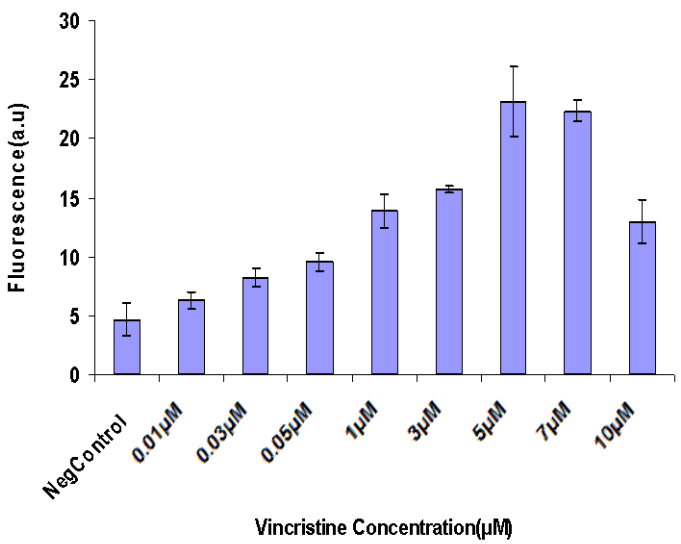

Figure 4 Expression level of bcl-2 shown as increase in the fluorescence, due to the treatment of different concentrations of vincristine in A549 cells determined by flow cytometry.

Conclusion

The Raman analysis confirms that vincristine interacts with the nuclear DNA resulting in significant changes to the spectroscopic markers of DNA which are characteristic of both intercalation and external binding. Changes observed in the DNA related features include those of cytosine (783 cm^{-1}), guanine (1318 cm^{-1}), thymine (1375 cm^{-1}), O-P-O of DNA (1095 cm^{-1}). Notably, the changes in the B-form DNA (827 cm^{-1}) in favour of A-form conformation and B-form DNA (1422 cm^{-1}) are prominent and systematic as a function of vincristine exposure. These changes can be taken as the Raman markers of DNA intercalation.

Expression of bcl-2 in A549 cells as a result of exposure to vincristine is found to be concentration dependant and increases with increasing concentration to a maximum, whereafter levels are reduced at higher doses. The up-regulation of bcl-2 is the response of the cell to the external agent which causes damage to the DNA and affects an inhibition of apoptosis. In the current study, the Raman spectral data indicated that vincristine binds the cellular DNA by intercalation, so here bcl-2 up regulation is in response to the DNA damage caused by the drug and confirms the findings of the Raman study for the interaction of this drug with nucleus of the A549 cells. Nevertheless, the MTT assay clearly indicates loss of viability at these doses, pointing to microtubule damage as the primary mode of action in this region. The study demonstrates the potential of Raman spectroscopy, not only for the fingerprinting and screening of cellular responses but for the elucidation of mechanisms of action of external agents.

Acknowledgements

The authors acknowledge funding through the Technology Sector Research (Strand III) programme of the Irish Higher Education Authority and the Irish HEA Programme for Research in Third Level Institutions, Cycle 4 National Biophotonics and Imaging Platform for Ireland (NBIPI), supported by the European Union Structural Fund.

References

1. C. A. Owen, J. Selvakumaran, I. Notingher, G. Jell, L. L. Hench and M. M. Stevens, *Journal of Cellular Biochemistry*, 2006, **99**, 178-186.
2. H. Nawaz, F. Bonnier, P. Knief, O. Howe, F. M. Lyng, A. D. Meade and H. J. Byrne, *Analyst*, 2010, **135**, 3070-3076.
3. H. Nawaz, F. Bonnier, A. D. Meade, F. M. Lyng and H. J. Byrne, *Analyst*, 2011, **136**, 2450-2463.
4. F. M. Lyng, E. O. Faolain, J. Conroy, A. D. Meade, P. Knief, B. Duffy, M. B. Hunter, J. M. Byrne, P. Kelehan and H. J. Byme, *Experimental and Molecular Pathology*, 2007, **82**, 121-129.
5. J. Chan, S. Fore, S. Wachsman-Hogiu and T. Huser, *Laser Photon. Rev.*, 2008, **2**, 325-349.
6. T. Huser, C. A. Orme, C. W. Hollars, M. H. Corzett and R. Balhorn, *J. Biophotonics*, 2009, **2**, 322-332.
7. P. Knief, C. Clarke, E. Herzog, M. Davoren, F. M. Lyng, A. D. Meade and H. J. Byrne, 2009.
8. A. D. Meade, C. Clarke, F. Draux, G. D. Sockalingum, M. Manfait, F. M. Lyng and H. J. Byrne, *Anal. Bioanal. Chem.*, 2010, **396**, 1781-1791.
9. A. D. Meade, F. M. Lyng, P. Knief and H. J. Byrne, *Anal Bioanal Chem*, 2007, **387**, 1717-1728.
10. J. Dorney, F. Bonnier, A. Garcia, A. Casey, G. Chambers and H. J. Byrne, *Analyst*, 2012, **137**, 1111-1119.
11. F. Draux, P. Jeannesson, A. Beljebbar, A. Tfayli, N. Fourre, M. Manfait, J. Sule-Suso and G. D. Sockalingum, *Analyst*, 2009, **134**, 542-548.
12. M. E. Keating, F. Bonnier and H. J. Byrne, *Analyst*, 2012, **137**, 5792-5802.
13. J. Ling, S. D. Weitman, M. A. Miller, R. V. Moore and A. C. Bovik, *Applied optics*, 2002, **41**, 6006-6017.
14. J. Y. Ling, Q. Z. Yang, S. S. Luo, Y. Li and C. K. Zhang, *Chinese Chemical Letters*, 2005, **16**, 71-74.
15. I. Notingher, *Sensors*, 2007, **7**, 1343-1358.
16. S. Verrier, I. Notingher, J. M. Polak and L. L. Hench, 2004.
17. Y. Yang, J. Sule-Suso, G. D. Sockalingum, G. Kegelaer, M. Manfait and A. J. El Haj, *Biopolymers*, 2005, **78**, 311-317.
18. L. Wilson and M. A. Jordan, *Chemistry & Biology*, 1995, **2**, 569-573.
19. Y. Zhu, H. Zeng, J. M. Xie, L. Ba, X. Gao and Z. H. Lu, *Microscopy and Microanalysis*, 2004, **10**, 286-290.
20. H. W. Tang, Y. Ye, T. Li, J. S. Zhou and G. Q. Chen, *Analyst*, 2003, **128**, 974-979.
21. G. Tyagi, D. K. Jangir, P. Singh and R. Mehrotra, *DNA and cell biology*, 2010.
22. A. Beham, M. C. Marin, A. Fernandez, J. Herrmann, S. Brisbay, A. M. Tari, G. Lopez-Berestein, G. Lozano, M. Sarkiss and T. J. McDonnell, *Oncogene*, 1997, **15**, 2767-2772.
23. E. Stephanova, T. Topouzova-Hristova and R. Konakchieva, *Toxicol In Vitro*, 2008, **22**, 688-694.
24. T. Mosmann, *Journal of Immunological Methods*, 1983, **65**, 55-63.
25. A. D. Meade, C. Clarke, F. Draux, G. D. Sockalingum, M. Manfait, F. M. Lyng and H. J. Byrne, *Anal Bioanal Chem*, 2010, **DOI: 10.1007/s00216-009-3411-7**.
26. F. E. Grubbs, *Technometrics*, 1969, **11**, 1-&.
27. H. Martens and M. Martens, 2000.
28. A. D. Meade, H. J. Byrne and F. M. Lyng, *Mutation Research-Reviews in Mutation Research*, 2010, **704**, 108-114.
29. F. Westad and H. Martens, *Journal of near Infrared Spectroscopy*, 2000, **8**, 117-124.
30. J. De Gelder, K. De Gussem, P. Vandenabeele and L. Moens, *Journal of Raman Spectroscopy*, 2007, **38**, 1133-1147.
31. P. R. T. Jess, V. Garces-Chavez, D. Smith, M. Mazilu, L. Paterson, A. Riches, C. S. Herrington, W. Sibbett and K. Dholakia, *Optics Express*, 2006, **14**, 5779-5791.
32. I. Notingher, S. Verrier, S. Haque, J. M. Polak and L. L. Hench, *Biopolymers*, 2003, **72**, 230-240.
33. K. Yuzaki and H. O. Hamaguchi, *Journal of Raman Spectroscopy*, 2004, **35**, 1013-1015.
34. G. J. Thomas, J. M. Benevides, S. A. Overman, T. Ueda, K. Ushizawa, M. Saitoh and M. Tsuboi, *Biophysical Journal*, 1995, **68**, 1073-1088.
35. J. M. Benevides, J. Kawakami and G. J. Thomas, *Journal of Raman Spectroscopy*, 2008, **39**, 1627-1634.
36. J. M. Benevides and G. J. Thomas, *Biochemistry*, 2005, **44**, 2993-2999.
37. M. Tsuboi, J. M. Benevides and G. J. Thomas, *Biophysical Journal*, 2007, **92**, 928-934.
38. J. C. Huang, D. B. Zamble, J. T. Reardon, S. J. Lippard and A. Sancar, *Proceedings of the National Academy of Sciences of the United States of America*, 1994, **91**, 10394-10398.
39. Ä. b. Karaman, E. M. Qannari, H. Martens, M. S. Hedemann, K. E. B. Knudsen and A. Kohler, *Chemometrics and Intelligent Laboratory Systems*, 2013, **122**, 65-77.
40. C. Borner, *Molecular immunology*, 2003, **39**, 615-647.

41. M. G. Vander Heiden and C. B. Thompson, *Nature cell biology*, 1999, **1**, E209-216.
42. S. A. Park, H. J. Park, B. I. Lee, Y. H. Ahn, S. U. Kim and K. S. Choi, *Brain research*, 2001, **93**, 18-26.
43. S. Singh, R. R. Chhipa, M. V. Vijayakumar and M. K. Bhat, *Cancer Letters*, 2006, **236**, 213-221.
44. H. K. Bojes, P. K. Suresh, E. M. Mills, D. R. Spitz, J. E. Sim and J. P. Kehrer, *Toxicol Sci*, 1998, **42**, 109-116.
45. P. A. Sotiropoulou, A. Candi, G. Mascre, S. De Clercq, K. K. Youssef, G. Lapouge, E. Dahl, C. Semeraro, G. Denecker, J. C. Marine and C. Blanpain, *Nature cell biology*, 2010, **12**, 572-U121.

Supplementary information:

Spectral ranges (cm^{-1})	assignments
621-626	C-C twisting of phenyl
629-633	C-C stretching
635-637	C-C stretching
637-643	C-C stretching of tyrosine residues
655-656	alanine
673-678	thymine
696-700	tryptophan ring breathing
703-704	tryptophan
708-711	tyrosine
719-727	Adenine/tryptophan
733-737	thymine
748-750	thymine
763-766	thymine
769-773	alanine
773-778	tryptophan
784-795	cytosine
797-808	O-P-O of DNA (A-form)
828-829	O-P-O of DNA (B-form)
842-844	CH in plane bending of tyrosine
849-857	C-C stretching
861-864	tryptophan
893-898	Deoxiribose of DNA
904-906	valine
936-939	C-C stretching
944-947	valine
1000-1007	Phenyl alanine

1021-1026	CH in plane bending
1030-1033	CH in plane bending
1055-1058	C-N stretching
1062-1065	O-P-O of the DNA
1075-1090	O-P-O of the DNA
1114-1121	C-N stretching
1142-1148	C-C stretching
1166-1173	cytosine
1176-1177	CH in plane bending of tyrosine
1194-1196	tyrosine
1209-1211	guanine
1251-1257	thymine
1250-1256	amide-III
1261-1261	Amide-III β-sheet
1263-1271	Amide-III β-sheet
1276-1280	Amide-III α-sheet
1289-1309	cytosine
1320-1322	guanine
1331-1332	tryptophan
1347-1360	CH_3 stretching
1340-1343	CH deformation
1378-1381	thymine
1424-1428	CH deformation
1453-1461	CH deformation
1468-1470	histidine
1503-1505	C=C stretching
1545-1559	tryptophan
1566-1572	tryptophan
1596-1597	C=C bending
1631-1633	histidine
1643-1645	C=C stretching
1663-1665	amide-I

1702-1709	thymine
1727-1731	C=O ester
1783-1786	C-C bending